archaeometry

*Archaeometry* **60**, 5 (2018) 1062–1076 doi: 10.1111/arcm.12369

# RAMAN SPECTROSCOPY AND SCANNING ELECTRON MICROSCOPY CONFIRM OCHRE RESIDUES ON 71 000-YEAR-OLD BIFACIAL TOOLS FROM SIBUDU, SOUTH AFRICA

M. WOJCIESZAK† and L. WADLEY

*Evolutionary Studies Institute (ESI), University of the Witwatersrand, Private Bag 3, Johannesburg 2050, South Africa*

*Micro-residue analysis of stone tools is generally performed with optical light microscopy and the visual observations are then compared with experimental, replicated pieces. This paper complements such archaeological research by providing physico-chemical evidence. Raman spectroscopy and scanning electron microscopy have been used to confirm the presence of hematite on red-stained medial and proximal parts of 71 000-year-old Still Bay bifacial tools from Sibudu Cave. Our results confirm the conclusion from optical light microscopy that the tools were hafted with an ochre-loaded adhesive. However, we point to some instances when hematite residues are incidental or may be inclusions in the rock used to make the stone tools.*

*KEYWORDS:* RESIDUES, STONE TOOLS, MIDDLE STONE AGE, RAMAN SPECTROSCOPY, OCHRE, SCANNING ELECTRON MICROSCOPY, STILL BAY

## INTRODUCTION

In Stone Age archaeological contexts, prolific numbers of stone tools are recovered and in many instances they are the only artefact type preserved. They can give much information about the behaviour of those who were using them. The tracking of geological sources informs us about people's movements. The investigation of knapping strategies gives clues to the type of technologies used. Use-wear and micro-residue analyses of stone tools help to explain the uses of tools and the composition of their hafting materials.

In South Africa, numerous archaeological sites have extensive stone artefact archives. Sibudu is one of these; it is a large rock shelter located in northern KwaZulu-Natal, about 40 km north of Durban. It was occupied sporadically between 77 000 and 38 000 years ago and its cultural sequence is mostly Middle Stone Age (MSA), although there is a long hiatus of occupation between 38 000 years ago and about 1000 years ago, when the final occupation was in the Iron Age (Wadley and Jacobs 2006). The technological industries represented in Sibudu's MSA are the pre–Still Bay, Still Bay, Howiesons Poort and post–Howiesons Poort. Various examples of innovative technology were discovered at Sibudu, such as insecticidal bedding construction (Wadley *et al*. 2011), preparation of compound adhesive and paint (Wadley *et al*. 2004, 2009; Villa *et al*. 2015; Rots *et al*. 2017) and diverse bone (Backwell *et al*. 2008; d'Errico *et al*. 2012) and stone technologies (Wadley 2005, 2007; Will *et al*. 2014; Soriano *et al*. 2015).

At Sibudu, the Still Bay Industry, the subject of this paper, has an age of 71 000 years ago (Jacobs *et al*. 2008) and it is characterized by double-pointed, bifacial foliate points (Wadley 2007). The bifacial points were produced by direct percussion by hard hammer,

*Received 24 February 2017; accepted 16 November 2017
†Corresponding author: email marine.wojcieszak@gmail.com

followed by thinning and retouch by soft stone hammer (Soriano *et al*. 2015). Some lithics in Still Bay were knapped with nodules of iron oxide that were used as soft hammers for retouching the tools (Soriano *et al*. 2009). Optical light microscopy analysis revealed the presence of mineral and organic (faunal and vegetal) residues on the tools (Lombard 2006b). The analysed tools were thought to have been hafted to wooden handles or shafts, and used as butchering knives or spearheads. The presence of ochre micro-residues on the bases of some points suggests that ochre powder was mixed into the adhesives, possibly as a loading agent. At Sibudu, ochre was also present in the adhesives used on post–Howiesons Poort points and Howiesons Poort segments (Lombard 2005, 2006a; Wadley *et al*. 2009). Until now, no chemical tests have been conducted on the Still Bay tool residues, so our aim here is to investigate the residues using Raman spectroscopy.

Raman spectroscopy produces information on the molecular composition, and the measurements are performed using milligram amounts of sample without destroying or even touching the samples. This technique is thus suitable for analysing micro-residues on archaeological artefacts. Fourier transform – infrared reflectance spectroscopy (FT–IR) has already been used successfully to identify organic micro-residues on archaeological (Zupancich *et al*. 2016) and replicated stone tools (Prinsloo *et al*. 2014). In this paper, we demonstrate the feasibility of using Raman microscopy to analyse archaeological stone tools and the mineral micro-residues present on them.

## MATERIALS AND METHODS

### *Pointed artefacts and sediments*

Six bifacial stone tools or fragments of tools from the 71 000-year-old Still Bay layers, RGS (Reddish Grey Sand) and RGS2, described elsewhere (Lombard 2006b; Wadley 2007), were selected for the chemical analysis. A sediments sample was taken from RGS and another from RGS2 to represent the soil environments from which the tools were excavated. The rocks from which the points were made are dolerite and quartzite.

The same nomenclature as in Lombard (2006b) is used here (Fig. 1):

- Tool 1: dolerite double-pointed, asymmetrical bifacial point.
- Tool 4: quartzite pointed proximal/medial fragment.
- Tool 5: dolerite pointed proximal/medial fragment.
- Tool 7: dolerite pointed proximal/medial fragment.
- Tool 8: quartzite diagonally fractured point.
- Tool 9: dolerite distal point fragment.

The artefacts were excavated by Marlize Lombard and placed into individual airtight plastic bags directly after their removal from the site sediment. They were not handled or removed from the bags until they were analysed in a clean microscopy laboratory. During microscopy, the residues were not touched or removed from the tools. However, after this residue analysis (for the residues identified, see Fig. S1), the tools were extensively handled while they were being studied and drawn by lithic technologists. At least three researchers handled the artefacts. The samples are stored inside individual plastic bags under room conditions at the Evolutionary Studies Institute. The residue analysis performed with optical light microscopy (Lombard 2006b) revealed faunal, vegetal and/or mineral residue types. Sediment from both RGS (excavated on 17 November 2008—square B4d) and RGS2 (excavated on 17 February 2018—square B4a) were also analysed by Raman spectroscopy.

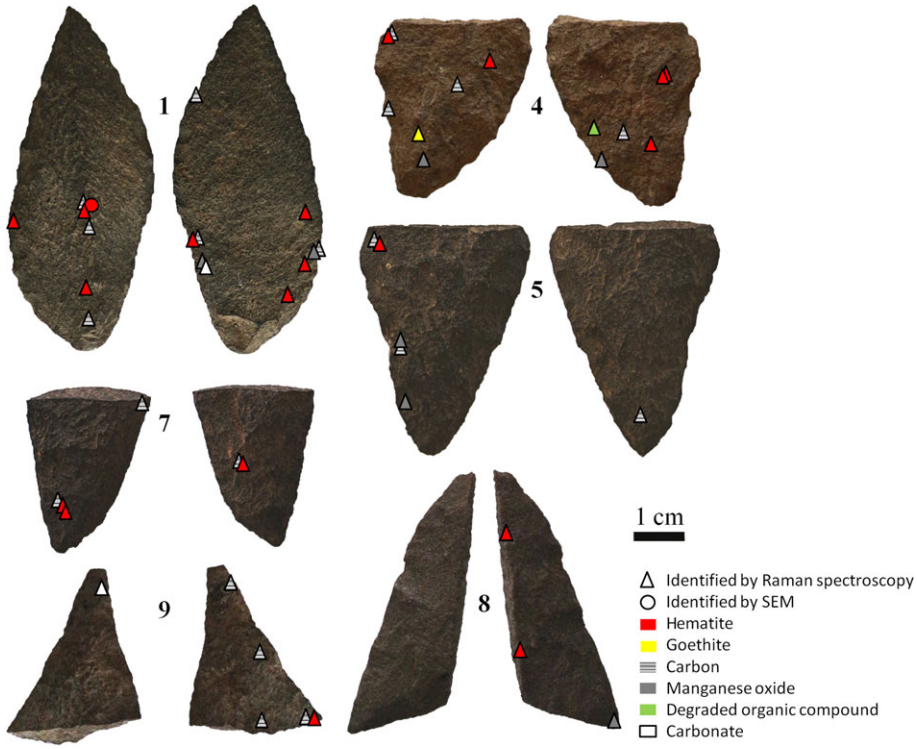


Figure 1 *Still Bay pointed artefacts from Sibudu Cave and micro-residue plots from Raman spectroscopy and scanning electron microscopy. [Colour figure can be viewed at wileyonlinelibrary.com]*

## *Methods*

*Raman spectroscopy* Raman micro-spectroscopy was undertaken using a LabRam HR800 (Horiba-Jobin Yvon) characterized by a local length of 800 mm and equipped with the 514.5 nm line of a Lexel argon ion laser and a 600 lines per millimetre grating (resolution $< 2\,cm^{-1}$). A pair of 50× and a 100× long working distance microscope objectives condensed the laser beam on to the sample and collected the backscattered Raman signal. The spectra were collected with a charge coupled detector (CCD) cooled with liquid nitrogen. The laser power was reduced using an optical filter to approximately 0.8 mW at the sample. Low laser power was used to avoid inducing thermal changes to the mineralogy of the iron and manganese oxide minerals. The integration time depended on the point of analysis and the level of fluorescence.

Raman was undertaken on dolerite and quartzite (the rocks from which the tools were made), the stone tool residues from all six tools and on two sediment samples from layers associated with the tools.

*Scanning electron microscopy* Secondary electron and backscattered electron images were obtained with a FEI Quanta 200 ESEM. It uses a conventional tungsten electron source, giving a resolution of 3.5 nm. The accelerating voltage used to observe the tools was 30 kV. The samples were observed (without preparation) on a metal support at high vacuum, with a working distance of approximately 10 mm. Energy-dispersive spectrometry (EDS) was also performed on the

samples in order to identify the elemental distribution of the points of interest either as single spots or in small areas. The same parameters as for the SEM were used and the element used for optimization was copper. SEM and EDS were only performed on Tools 1 and 4.

*Optical microscopy* An Olympus BX63 upright microscope with reflective light and CellSem Dimension software were used to record images of the surface of the tools. Magnification objectives of 5× and 20× obtained images with the *z*-stacking option of the software.

## RESULTS AND DISCUSSION

Fluorescence is one of the major limiting factors when analysing archaeological materials with Raman spectroscopy and most locations where analysis was performed on the Sibudu tools showed only a fluorescence signal. As a result, many locations had to be tested on each tool to obtain good-quality Raman spectra. We now discuss the various types of spectra obtained by Raman: first, those from contaminants, second, those from minerals present in the rocks from which the points were made; and, third, from residues on the tools, such as ochre, amorphous carbon, manganese oxides and degraded organic compounds. In the ochre section, we include results obtained from scanning electron microscopy and semi-quantitative EDS. We discuss the results of the sediment sample analysis under 'Contaminants' because the sediment from which the tools were excavated is likely to be present on them, yet it does not represent use-related residue.

### *Contaminants*

When performing micro-residue analysis, contaminants have to be taken into account to exclude them from the final interpretation of use-related residues. The contamination can be modern, ancient or post-depositional (though possibly still ancient). Even if special care is taken during excavation and post-excavation treatment, if the subsequent work is not performed under cleanroom conditions, the possibility of modern contamination has to be considered when tools are analysed at high magnifications. Several types of modern contamination have previously been identified on replicated and archaeological stone tools (Wadley and Lombard 2007; Pedergnana *et al*. 2016). Vegetal contaminants are usually dominant, such as plant fibres, cellulose tissues, spores and pollen, but they can also be faunal, such as hair or feather (Wadley and Lombard 2007) (Fig. 1).

Figure 2 (a) presents a backscattered electron image of a 90 µm diameter fibre on Tool 1. The colour contrast generated on the backscattered electron images allows an easy detection of animal and vegetal fibres present on the surface of stone materials. EDS analysis was not possible because these fibres move under exposure to the beam. Pedergnana *et al*. (2016) observed similar types of fibres on their replicated stone tools and noted that a slight twist of the fibre is frequently observed for ancient fibres. However, the fibre shown in Figure 2 (a) is sitting on the top of the tool and does not look degraded. This fibre is thus most probably a modern vegetal fibre contaminant that was deposited on the tool from the air.

A mixed spectrum of quartz, feldspar and a carbonate (data not shown) was recorded on the proximal part of Tool 1 (see Fig. 1). The carbonate band occurs at 1085 $cm^{-1}$, which can be characteristic of calcite. This carbonate is probably contamination from the sediments in which the tools were buried. Raman analyses of two sediment samples from layers RGS and RGS2 show the presence of several mineral species including carbonates (Fig. 2 (b)). Calcite was

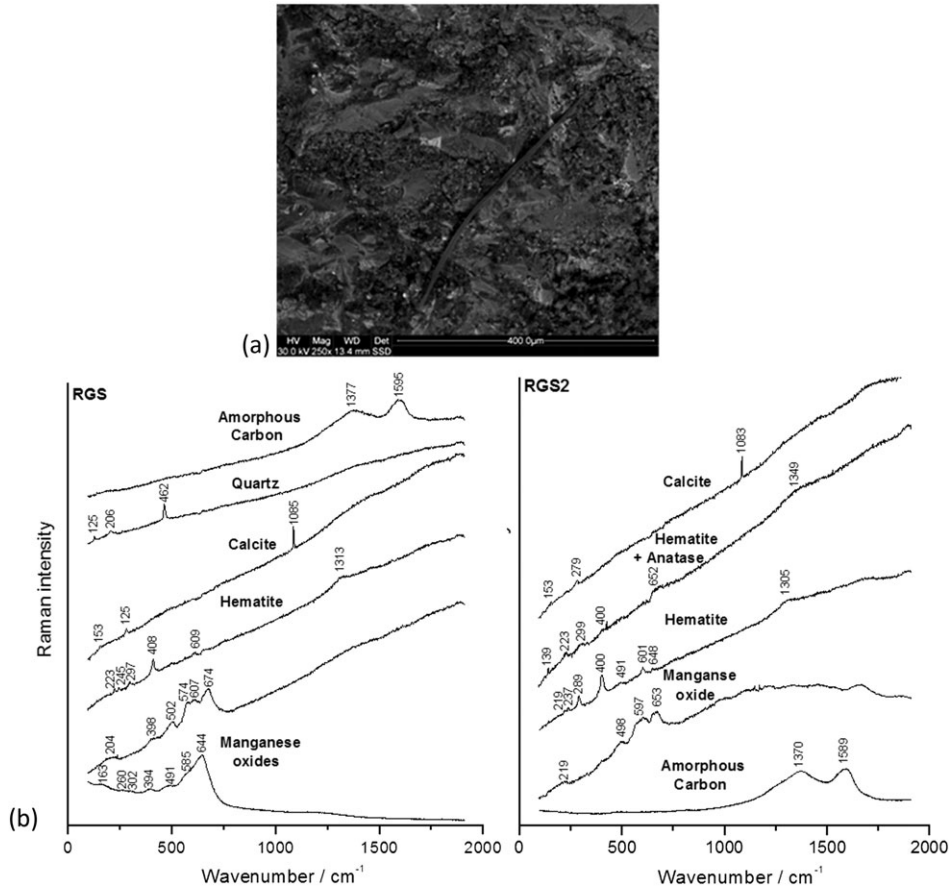


Figure 2 *(a) A backscattered electron image of a micro-fibre on Tool 1. (b) Raman spectra obtained from two Sibudu sediment samples: RGS (left) and RGS2 (right) layers.*

recorded in both samples, as well as amorphous carbon, which confirms that its presence on the tools can be accidental. Raman microanalysis also revealed spectra of quartz in the RGS and anatase in the RGS2 sediment. Three types of manganese oxides were detected in the sediments. It is not straightforward to distinguish the manganese oxides: manganese forms a large number of compounds in non-stoichiometric and disordered systems. One exhibits an intense Raman band at 644 $cm^{-1}$, which can be attributed to jacobsite and todorokite structure (De Benedetto *et al.* 2011). The second spectrum shows the Raman features of bixbyite ($\alpha$-$Mn_2O_3$) around 204, 398, 502 and 674 $cm^{-1}$, and two other Raman bands at 574 and 607 $cm^{-1}$ can be assigned to $MnO_2$ types (Buciuman *et al.* 1999; Smith *et al.* 1999; Julien *et al.* 2004; Froment *et al.* 2008). The last spectrum presented several broad Raman bands around 498, 597 and 653 $cm^{-1}$, which could not be attributed to a specific manganese oxide species; it is probably a mixture of them. The presence of manganese oxides in sediments is commonly due to bacterial activity, but it is, of course, not the only origin. Besides Mn in various forms, the sediment samples also contained hematite with the same characteristic bands described for the tools' residues. $Fe_2O_3$ is a quite common natural occurrence in sediments. Liedgren *et al.* (2017) conducted fire experiments to study the effects of heat on sediments; in the process, they discovered that iron oxide is a

particularly common product of heated sediment. In Sibudu, people processed a lot of ochre, and they also created many fires, so the presence of iron oxide in the sediments is to be expected.

### *Minerals present in the rock*

The Raman spectra of some mineral species identified in rocks used to make stone tools are shown stack plotted in Figure 3. For all samples, except Tool 9, quartz was detected with bands at 465, 354, 264, 208 and 128 $cm^{-1}$ (Smith *et al.* 1999). Quartz spectra were obtained on every part of the tools. Quartz was thought to be mixed into complex paint or adhesive recipes at Blombos Cave (Henshilwood *et al.* 2011) and Diepkloof Rock Shelter (Charrié-Duhaut *et al.* 2013); quartz grains are also a natural inclusion in ochre fragments and in ochre powder when ochre is ground on grindstones with quartz inclusions (Wadley *et al.* 2009). Because of the numerous possible origins of quartz on the Sibudu tools, it is difficult—perhaps impossible—to distinguish use-related quartz inclusions from geological ones.

The Raman spectra recorded on points made of dolerite (Tools 1, 5, 7 and 9) reveal the presence of silicates other than quartz, such as pyroxene (Tool 5) and feldspar (Tools 1, 5 and 7). One pyroxene spectrum was also recorded on a quartzite sample (Tool 4). The pyroxene spectra exhibit bands at 149, 226, 382, 428, 527, 556, 665, 726 and 863 $cm^{-1}$ and a broad band around 1015 $cm^{-1}$. The weak band at 428 $cm^{-1}$ could be attributed to jadeite (Lafuente *et al.* 2015), a sodic pyroxene ($NaAlSi_2O_6$). All other bands are more similar to the spectra of ferromagnesian and calcic pyroxenes such as augite $(Ca,Na)(Mg,Fe,Al)(Al,Si)_2O_6$) (Makreski *et al.* 2006) or diopside

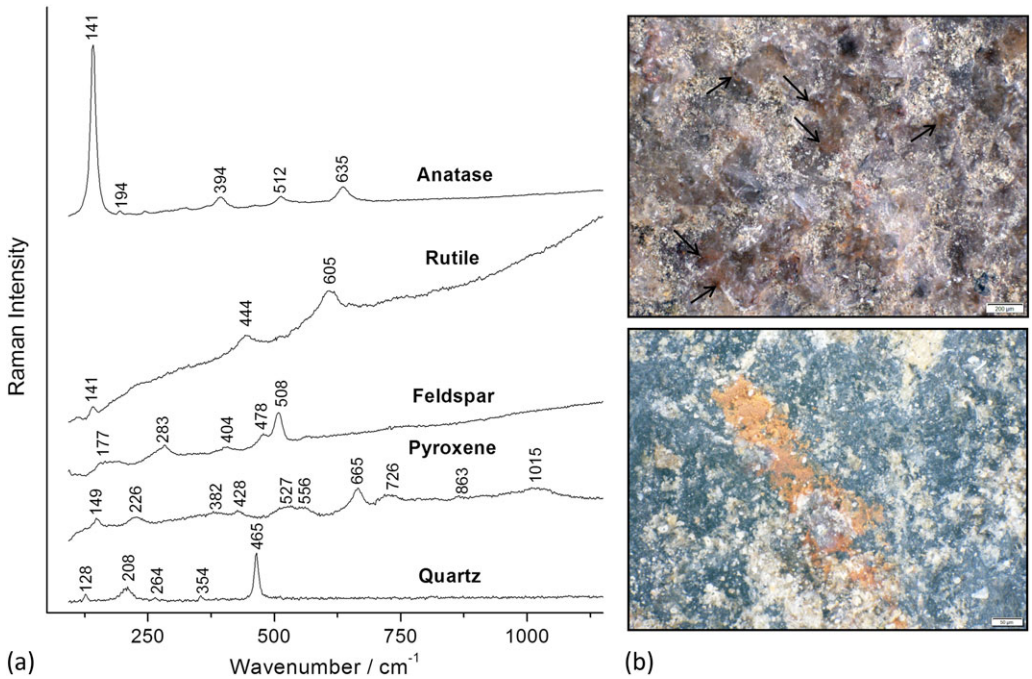


Figure 3 *(a) Raman spectra of mineral components of the rocks used for making the stone tools: quartz and pyroxene were recorded in both quartzite and dolerite artefacts, feldspar only on dolerite; and anatase and rutile only in quartzite-type tools. (b) Microscopic images recorded on Tool 8 (arrows showing red inclusions embedded within the rock—top) and on Tool 7 with red ochre powder pasted on the rock. [Colour figure can be viewed at wileyonlinelibrary.com]*

($Ca(Mg,Fe)Si_2O_6$) (Lafuente *et al*. 2015). The Raman features of feldspar are localized around 177, 283, 408, 482 and 508 $cm^{-1}$. Mernagh (1991) observed that feldspar can be distinguished using the bands around 200 and 300 $cm^{-1}$, and 500 $cm^{-1}$. For alkali feldspar spectra, a triplet is generally observed in the 450–600 $cm^{-1}$ region, while the plagioclases show mainly two intense bands. The feldspar spectra obtained on the tools are more likely to be plagioclase, such as oligoclase. Platy plagioclase grains are clearly seen in thin sections of dolerite from Sibudu (Wadley and Kempson 2011).

In addition, for Tool 4, a quartzite-based pointed fragment, two titanium dioxides ($TiO_2$) were detected. Rutile presents characteristic bands at 141, 444 and 605 $cm^{-1}$ and anatase at 141, 194, 394, 512 and 635 $cm^{-1}$ (Edwards *et al*. 2000). Anatase and rutile are common in igneous rocks. Rutile exhibits a reddish brown to red colour. By looking at the tools under optical light microscopy, many red areas are observable; rutile and hematite can easily be confused visually. Colour is thus not sufficient to corroborate the presence of hematite on the stone tools; hence the need to use molecular techniques of analysis such as Raman spectroscopy. However, another problem for residue analysts is that dolerite contains iron naturally, and in the geological specimens from the Sibudu area, this can be up to 14% of the major elements recorded by XRF (Wadley and Kempson 2011). Lombard (2006b) mentioned that ochre residues on tools can be confused with red iron-rich geological inclusions. Thus it is important to distinguish, visually, between iron oxide inclusions embedded within the rock (Fig. 3 (b), top) and hematite powder mixed with other ingredients and pasted on to the tool (Fig. 3 (b), bottom). We discuss the issue of context again later.

### *Ochre*

In Sibudu, 9286 ochre pieces were found in the MSA occupations (Hodgskiss 2012); it was a material that was used extensively at this site. What we refer to as ochre is rock (such as shale, sandstone, mudstone or specularite) that contains iron oxide (such as hematite) or oxyhydroxide (such as goethite), which leaves a reddish or yellowish streak. Many red ochre residues have been identified on Sibudu stone tools with the naked eye, or by optical light microscopy with a relatively low magnification (50–100×) (Wadley *et al*. 2004). Lombard (2006b) identified ochre residues in greater or lesser proportions on each of the Still Bay stone artefacts presented in this paper. These ochre traces mostly occur as hafting lines (concentrations of residues probably pushed together at the haft or binding terminations) on the medial portions of the tools, often on both ventral and dorsal faces. Consequently, the ochre was interpreted as an ingredient of adhesive used for attaching the stone tool to a shaft or handle.

Scanning electron microscopy and semi-quantitative EDS were performed on Tool 1. The results show the presence of iron and oxygen as major elements on the dark area present in Figure 4, suggesting the presence of iron oxide. The lighter area around the dark patch mostly comprises oxygen, silicium, aluminium and calcium, but also with traces of iron, magnesium and potassium, which can correspond to calcic pyroxenes. This iron oxide residue is on the hafting line identified by Lombard (2006b) so, as previously suggested, it may be part of the adhesive on the tool. The lighter area with calcium and aluminium may be part of the dolerite on which the stain rests.

Raman spectroscopy identified the features of hematite ($\alpha$-$Fe_2O_3$), located around 221–227, 243–247, 293–297, 402–415, 500–502, 603–618, 652–666 and 1303–1347 $cm^{-1}$ (de Faria *et al*. 1997; Colomban *et al*. 2001), on all the tools (an example of a spectrum is shown in Fig. 5 (a), bottom). One spectrum recorded on Tool 7 (Fig. 5 (a), middle) presents hematite peaks at

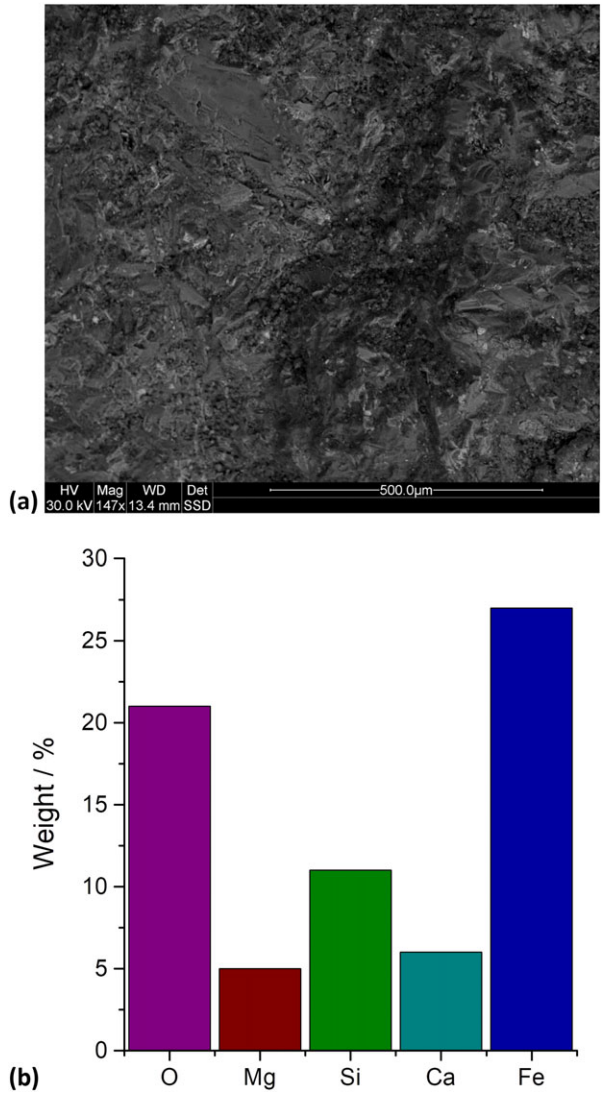


Figure 4 *(a) A backscattered electron image of Tool 1 and (b) semi-quantitative EDS analysis of the darker area, suggesting the presence of iron oxide. [Colour figure can be viewed at wileyonlinelibrary.com]*

219, 289, 404, 500, 610, 661 and 1330 $cm^{-1}$, but at a different band intensity ratio because of the anisotropic character of hematite crystals. Sometimes, the vibrational signature of hematite was mixed with other contributions from amorphous carbon or pyroxene. Almost all of the ochre occurrences recognized through microscopy by Marlize Lombard were confirmed as hematite using Raman spectroscopy and this can be seen by comparing our residue mapping with that of Lombard (2006b) (Figs 1 and S1). However, in some instances, only a fluorescence signal could be detected on those red residues, especially on Tools 5, 8 and 9. Random areas of the tools were tested as well as the areas where Lombard had observed ochre. Only Tool 4 yielded an additional residue; here, a spectrum of goethite was recorded (Fig. 5 (a), top), with bands at 90, 242, 298,

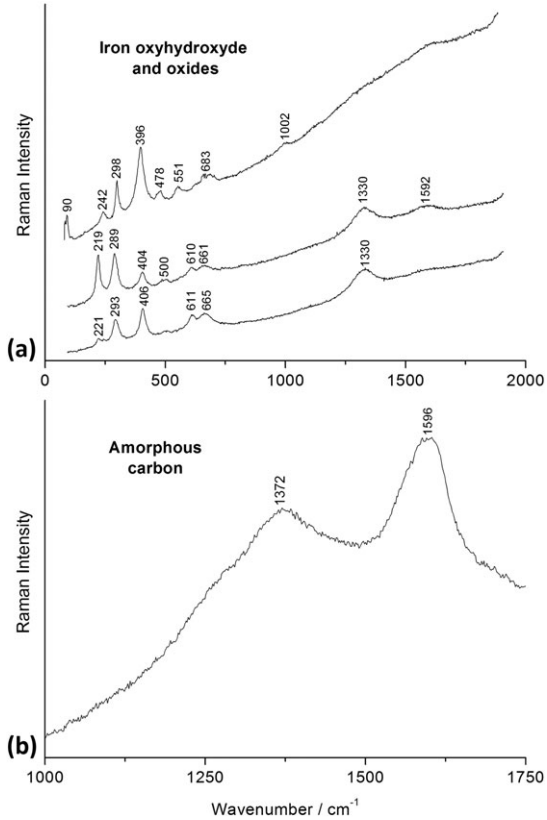


Figure 5 *(a) Raman spectra of a microscopic yellow area present on Tool 4 (top), a red micro-residue present on Tool 7 (middle) and typical hematite recorded on all the tools (bottom). (b) The Raman spectrum of amorphous carbon recorded on Tool 4.*

396, 478, 551, 683 and 1002 $cm^{-1}$ (de Faria *et al*. 1997; Smith *et al*. 1999). Geological ochre pieces collected about 1 km away from Sibudu often present mixtures of hematite and goethite (Wojcieszak and Hodgskiss; paper in preparation). Goethite could also be a weathering product and could have formed after the burying of the tool within the archaeological deposits. Tool 9 is a distal fragment and Tool 8 is a diagonally split tool that is largely a distal fragment. Neither would be expected to have traces of adhesive on them, yet, like Lombard, we saw a few red spots of hematite on these tools. We do not know the full size of these broken tools, but the break on Tool 9 may be close to the hafting line and this may explain the presence of one small ochre trace. The red ochre traces on Tool 8 may be contamination or red marks in the rock of the tool (see Fig. 3 (b), top). The presence of hematite in the sediment surrounding the tool implies that some ochre residues on the tools may be contaminants. However, the majority of the Sibudu hematite-bearing residues on Tools 1, 4, 5 and 7 (either recognized microscopically or by Raman) are localized on the medial and proximal parts of the tools, and these residues seem to be securely embedded (sometimes pasted) on the tool surfaces. This, and the restricted distribution of hematite on the stone tools, seems more likely to result from anthropogenic activities than accidental contamination, at least for Tools 1 and 4, which showed many hematite occurrences. Nonetheless, contamination can sometimes occur. Microscopy is best placed to identify superficial contamination because it is most

successfully recognized when, for example, an ochre trace lies on top of loose ash or sediment on a tool. On Tools 1, 5 and 7, hematite spectra were obtained on areas identified as ochre residues by Lombard (2006b). On Tool 4, a hematite spectrum was recorded on a residue called 'brown stain' by Lombard (2006b). Ochre colour depends on the mineralogy, crystal structure, particle size, inclusions and element substitutions within the hematite crystal lattice; it varies from red, yellow, orange or purple to brown. Raman spectroscopy highlighted the presence of hematite on brown stains that cannot visually be recognized as ochre, even microscopically. Different types or qualities of ochre may have been used for the preparation of adhesive and binding materials, or as abraders and hammers (Soriano *et al*. 2009). All ochre occurrences that were securely identified by Raman are localized on the medial/proximal parts of the tools and this gives credibility to the hypothesis of an ochre mixture used in the hafting process (Wadley 2005). Recently, in a new, independent study (Rots *et al*. 2017), ochre-loaded adhesive was also found on the medial and proximal portions of pressure-flaked serrate bifacial points at Sibudu, in layers that are older than 77 000 years ago. Rots and colleagues used SEM–EDS to identify some of the residues on the tools, but the use of Raman spectroscopy would have added more credibility to the study, since it gives direct evidence for molecular species. Microscopy is repeatedly criticized for being less accurate than physico-chemical studies of residues. The results presented here add clear evidence that some, but not all, microscopic observations of residues can be confirmed by methods such as Raman spectroscopy. On Tools 1 and 4, we were able to demonstrate clear evidence for spatial distribution of hematite that is most likely to have resulted from the use of hematite-loaded adhesive. While the distribution of hematite on Tools 5 and 7 is suggestive, we are cautious about claiming that they also bore hematite-loaded adhesive, because some hematite is present in the Sibudu sediments.

### *Amorphous carbon*

Raman spectra of amorphous carbon were recorded on all specimens (Fig. 5 (b)). The carbon is in localized patches, but it occurs on distal, medial and proximal portions of the tools; in other words, in random positions on the tools. The spectra exhibit two broad bands around 1363–1385 and 1595–1610 $cm^{-1}$. The first band (at a lower wavenumber), called the D band, is assigned to $sp^3$ carbon ($A_{1g}$ mode) (Smith *et al*. 1999; Hernanz *et al*. 2006). The second band (at a higher wavenumber), called the G band, is assigned to $sp^2$ carbon ($E_{2g}$ mode) (Smith *et al*. 1999; Hernanz *et al*. 2006). The G and D bands appear in poorly organized carbonaceous materials such as charcoal and soot. Bone or ivory black is excluded, since the phosphatic symmetric stretching mode near 960 $cm^{-1}$ was not observed. Amorphous carbon occurs in abundance in sediments, rocks and on archaeological artefacts from various sources. Many ancient camp fires were discovered in Sibudu, so charcoal on tools could come from accidental contact with hearths and hearth products. While our evidence implies that amorphous carbon occurs as part of a geological inclusion on the Sibudu tools, Iriarte *et al*. (2017) suggest that amorphous carbon may sometimes be an ingredient in pigment.

### *Manganese oxides*

For Tool 1 only, on tiny areas of the proximal portion, two spectra were recorded showing bands at 190, 405, 480, 512, 590, 650 and 745 $cm^{-1}$ (Fig. 6 (a), top spectrum). The spectral range between 500 and 700 $cm^{-1}$ is characteristic of Mn–O and Mn–OH bending and stretching vibrations (Ospitali *et al*. 2006). The band at 405 $cm^{-1}$ can be attributed to oxides with a poorly

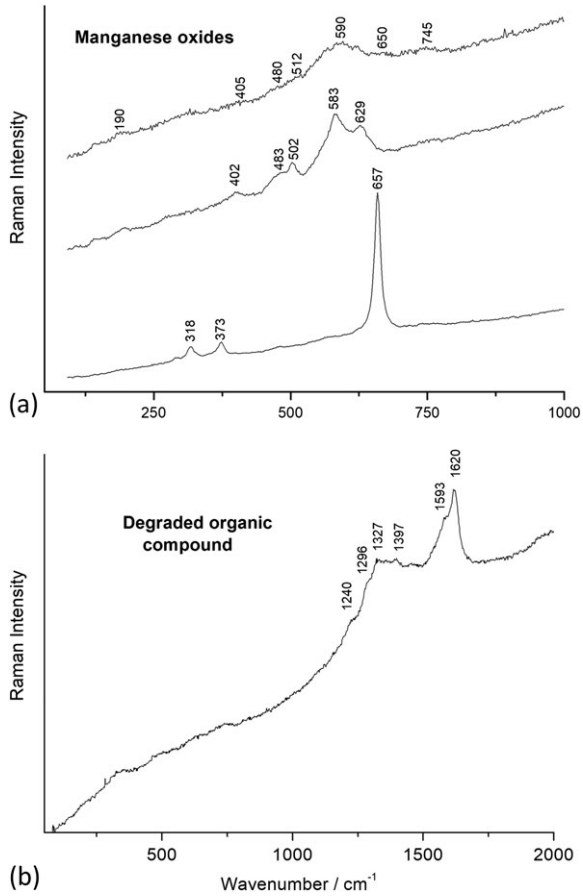


Figure 6 *(a) Raman spectra recorded in a microscopic black area on the proximal portion of Tool 1 (top), in microscopic dark brown areas on the proximal portion of Tool 4 (middle), and on Tools 4 and 5 (bottom). (b) A Raman spectrum of a degraded organic compound.*

crystalline structure, such as birnessite (Bruins *et al*. 2015). Julien *et al*. (2003) recognized three major features of birnessite-type $MnO_2$ at 500–510, 575–585 and 625–650 $cm^{-1}$ that match with spectra recorded on Tool 1. Birnessite is typical secondary manganese oxide (White *et al*. 2009; Frierdich *et al*. 2011). Another type of manganese oxide was recorded near the edge of Tool 4 (Fig. 6 (a), middle spectrum) and it presents two strong vibrational bands at 583 and 629 $cm^{-1}$, characteristic of β-$MnO_2$ (pyrolusite) (Widjaja and Sampanthar 2007). We also detected a further type of manganese oxide on Tools 4 and 5 (Fig. 6 (a), bottom spectrum), with a strong band at 657 $cm^{-1}$ and two weak features at 373 and 318 $cm^{-1}$, which are attributed to $Mn_3O_4$ (hausmanite) (Widjaja and Sampanthar 2007). However, the Raman features on the tools are different from the spectra recorded in the sediments, so the manganese oxide on the tools is unlikely to be from the sediment. The manganese oxides on the tools are most likely to be geological inclusions in the ochre and are, as such, unintentional residues. Manganese oxides were recorded on archaeological ochre pieces from Sibudu and Rose Cottage Caves (Wojcieszak and Hodgskiss; paper in preparation). The manganese oxide identified on the tools here always occurs on those portions of the tool where ochre also occurs.

*Degraded organic compound*

Raman spectroscopy studies of organic compounds on art objects or archaeological artefacts and their contexts pose more problems than for mineral compounds. Organic compounds form a family of complex chemical species, with a potential for extensive degradation, and a high level of fluorescence caused by the deterioration process. Depending on the period and the burial conditions of archaeological artefacts, organic compounds are susceptible to fossilization, which precludes their recognition using molecular and elemental techniques. Figure 6 (b) presents the Raman spectrum recorded on a ~1 μm diameter fibre on Tool 4. This fibre is embedded with other components, and is not sitting on the top of the tool like the one identified by SEM (Fig. 2 (a)). Thus, it is unlikely that this fibre comes from contamination. The Raman spectrum exhibits several components from 1240 to 1620 $cm^{-1}$. These features are most likely to be attributed to aromatic compounds probably coming from the degradation process of organic matter through heating (incomplete combustion of organic matter). Any kind of organic matter that is partially burnt could present those vibrational features before transforming to amorphous carbon. Lombard (2006b) identified a wood residue in this area of the tool (see Fig. S1). In this case, we can thus hypothesize that the residue is burnt vegetal fibre. Sometimes vegetal fibres are deliberately burnt: Ju/'hoan hunters from Nyae Nyae, near Tsumkwe in Namibia, use carbonized grass in the manufacture of plant fixative pastes (Wadley *et al*. 2015). If the Sibudu micro-residue does not represent pre- or post-depositional contamination, it could be a component in a composite adhesive made for hafting.

## CONCLUSION

Raman spectroscopy and microscopy are complementary methods for understanding the mineralogical composition and micro-residues on stone tools. However, microscopy alone will never be sufficient for the identification of hematite or the composition of red compounds. Not all hematite residues on Sibudu's Still Bay points observed with optical microscopy by Lombard (2006b) could also be detected with Raman, because of the fluorescence effect. Yet, Raman can sometimes identify hematite residues that were not visually detected; for example, the presence of ochre was confirmed in residues that, from microscopic observations, Lombard (2006b) classified as brown stains. Raman also reveals the presence of residues such as amorphous carbon and manganese oxides. Infrared spectroscopy analyses, often coupled with Raman spectroscopy, were performed to try to confirm the presence of organic residues on the tools. The analyses were conducted with a microscope in reflection mode; however, this form of analysis was not appropriate for the type of samples and the microscopic size of the residues. This chemical study has resulted in two important conclusions. First, it corroborates some of the observations made by microscopy on the Sibudu Still Bay points and it demonstrates the usefulness of microscopy as a first stage of residue analysis. Second, it conclusively establishes the use of ochre-loaded adhesives as a hafting methodology by in the Still Bay Industry in KwaZulu-Natal. The technological complexity involved in manufacturing compound adhesives that require careful assembly followed by precise pyrotechnology confirms other strands of evidence that suggest advanced technical behaviour of people by at least 71 000 years ago in Sibudu.

## ACKNOWLEDGEMENTS

The authors are grateful to Dr Rudolph Erasmus for access to the Raman spectrometer at the University of the Witwatersrand. The Microscopy and Microanalysis Unit (MMU) at the

university is also acknowledged for the use of the optical and electron microscopes. The authors acknowledge the MONARIS laboratory (Paris, UPMC) for allowing the IR tests on the tools. A temporary export permit (#2444) for the six tools was obtained from SAHRA, but the tools are now at the University of the Witwatersrand, in the Evolutionary Studies Institute. The support of the DST–NRF Centre of Excellence in Palaeosciences (CoE in Palaeosciences) towards this research is hereby acknowledged. LW is funded by an African Origins Platform grant from the National Research Foundation (NRF), South Africa. The opinions expressed, and conclusions arrived at, are those of the authors and are not necessarily to be attributed to the CoE in Palaeosciences, or the NRF. Drawings by Lombard included in Figure S1 were reproduced with the permission of Southern African Humanities. The authors also thank the two anonymous reviewers for their comments and suggestions, which helped to improve the final manuscript.

## REFERENCES

Backwell, L., d'Errico, F., and Wadley, L., 2008, Middle Stone Age bone tools from the Howiesons Poort layers, Sibudu Cave, South Africa, *Journal of Archaeological Science*, **35**(6), 1566–80.

Bruins, J. H., Petrusevski, B., Slokar, Y. M., Kruithof, J. C., and Kennedy, M. D., 2015, Manganese removal from groundwater: characterization of filter media coating, *Desalination & Water Treatment*, **55**(7), 1851–63.

Buciuman, F., Patcas, F., Craciun, R., and Zahn, D. R. T., 1999, Vibrational spectroscopy of bulk and supported manganese oxides, *Physical Chemistry Chemical Physics*, **1**(1), 185–90.

Charrié-Duhaut, A., Porraz, G., Cartwright, C. R., Igreja, M., Connan, J., Poggenpoel, C., and Texier, P.-J., 2013, First molecular identification of a hafting adhesive in the Late Howiesons Poort at Diepkloof Rock Shelter (Western Cape, South Africa), *Journal of Archaeological Science*, **40**(9), 3506–18.

Colomban, P., Sagon, G., and Faurel, X., 2001, Differentiation of antique ceramics from the Raman spectra of their coloured glazes and paintings, *Journal of Raman Spectroscopy*, **32**(5), 351–60.

d'Errico, F., Backwell, L. R., and Wadley, L., 2012, Identifying regional variability in Middle Stone Age bone technology: the case of Sibudu Cave, *Journal of Archaeological Science*, **39**(7), 2479–95.

De Benedetto, G. E., Nicolì, S., Pennetta, A., Rizzo, D., Sabbatini, L., and Mangone, A., 2011, An integrated spectroscopic approach to investigate pigments and engobes on pre-Roman pottery, *Journal of Raman Spectroscopy*, **42**(6), 1317–23.

de Faria, D. L. A., Venâncio Silva, S., and de Oliveira, M. T., 1997, Raman microspectroscopy of some iron oxides and oxyhydroxides, *Journal of Raman Spectroscopy*, **28**(11), 873–8.

Edwards, H. G. M., Newton, E. M., and Russ, J., 2000, Raman spectroscopic analysis of pigments and substrata in prehistoric rock art, *Journal of Molecular Structure*, **550–1**, 245–56.

Frierdich, A. J., Hasenmueller, E. A., and Catalano, J. G., 2011, Composition and structure of nanocrystalline Fe and Mn oxide cave deposits: implications for trace element mobility in karst systems, *Chemical Geology*, **284**(1–2), 82–96.

Froment, F., Tournié, A., and Colomban, P., 2008, Raman identification of natural red to yellow pigments: ochre and iron-containing ores, *Journal of Raman Spectroscopy*, **39**(5), 560–8.

Henshilwood, C. S., d'Errico, F., van Niekerk, K. L., Coquinot, Y., Jacobs, Z., Lauritzen, S.-E., Menu, M., and García-Moreno, R., 2011, A 100,000-year-old ochre-processing workshop at Blombos Cave, South Africa, *Science*, **334**(6053), 219–22.

Hernanz, A., Mas, M., Gavilán, B., and Hernández, B., 2006, Raman microscopy and IR spectroscopy of prehistoric paintings from Los Murciélagos cave (Zuheros, Córdoba, Spain), *Journal of Raman Spectroscopy*, **37**(4), 492–7.

Hodgskiss, T., 2012, An investigation into the properties of the ochre from Sibudu, KwaZulu-Natal, South Africa, *Southern African Humanities*, **24**, 99–120.

Iriarte, M., Hernanz, A., Gavira-Vallejo, J. M., Alcolea-González, J., and de Balbín-Behrmann, R., 2017, μ-Raman spectroscopy of prehistoric paintings from the El Reno cave (Valdesotos, Guadalajara, Spain), *Journal of Archaeological Science: Reports*, **14**, 454–60.

Jacobs, Z., Roberts, R. G., Galbraith, R. F., Deacon, H. J., Grün, R., Mackay, A., Mitchell, P., Vogelsang, R., and Wadley, L., 2008, Ages for the Middle Stone Age of Southern Africa: implications for human behavior and dispersal, *Science*, **322**(5902), 733–5.

Julien, C., Massot, M., Baddour-Hadjean, R., Franger, S., Bach, S., and Pereira-Ramos, J. P., 2003, Raman spectra of birnessite manganese dioxides, *Solid State Ionics*, **159**(3–4), 345–56.

Julien, C. M., Massot, M., and Poinsignon, C., 2004, Lattice vibrations of manganese oxides, part I: periodic structures, *Spectrochimica Acta Part A: Molecular and Biomolecular Spectroscopy*, **60**(3), 689–700.

Lafuente, B., Downs, R. T., Yang, H., and Stone, N., 2015, The power of databases: the RRUFF project, in *Highlights in mineralogical crystallography* (eds. T. A. and R. M. Danisi), 1–30, De Gruyter, Berlin.

Liedgren, L., Hörnberg, G., Magnusson, T., and Östlund, L., 2017, Heat impact and soil colors beneath hearths in northern Sweden, *Journal of Archaeological Science*, **79**, 62–72.

Lombard, M., 2005, Evidence of hunting and hafting during the Middle Stone Age at Sibidu Cave, KwaZulu-Natal, South Africa: a multianalytical approach, *Journal of Human Evolution*, **48**(3), 279–300.

Lombard, M., 2006a, Direct evidence for the use of ochre in the hafting technology of Middle Stone Age tools from Sibudu Cave, *Southern African Humanities*, **18**(1), 57–67.

Lombard, M., 2006b, First impressions of the functions and hafting technology of Still Bay pointed artefacts from Sibudu Cave, *Southern African Humanities*, **18**(1), 27–41.

Makreski, P., Jovanovski, G., Gajović, A., Biljan, T., Angelovski, D., and Jaćimović, R., 2006, Minerals from Macedonia, XVI: vibrational spectra of some common appearing pyroxenes and pyroxenoids, *Journal of Molecular Structure*, **788**(1–3), 102–14.

Mernagh, T. P., 1991, Use of the laser Raman microprobe for discrimination amongst feldspar minerals, *Journal of Raman Spectroscopy*, **22**(8), 453–7.

Ospitali, F., Smith, D. C., and Lorblanchet, M., 2006, Preliminary investigations by Raman microscopy of prehistoric pigments in the wall-painted cave at Roucadour, Quercy, France, *Journal of Raman Spectroscopy*, **37**(10), 1063–71.

Pedergnana, A., Asryan, L., Fernández-Marchena, J. L., and Ollé, A., 2016, Modern contaminants affecting microscopic residue analysis on stone tools: a word of caution, *Micron*, **86**, 1–21.

Prinsloo, L. C., Wadley, L., and Lombard, M., 2014, Infrared reflectance spectroscopy as an analytical technique for the study of residues on stone tools: potential and challenges, *Journal of Archaeological Science*, **41**, 732–9.

Rots, V., Lentfer, C., Schmid, V. C., Porraz, G., and Conard, N. J., 2017, Pressure flaking to serrate bifacial points for the hunt during the MIS5 at Sibudu Cave (South Africa), *PLOS ONE*, **12**(4), e0175151.

Smith, D. C., Bouchard, M., and Lorblanchet, M., 1999, An initial Raman microscopic investigation of prehistoric rock art in caves of the Quercy District, S.W. France, *Journal of Raman Spectroscopy*, **30**(4), 347–54.

Soriano, S., Villa, P., and Wadley, L., 2009, Ochre for the toolmaker: shaping the Still Bay Points at Sibudu (KwaZulu-Natal, South Africa), *Journal of African Archaeology*, **7**(1), 41–54.

Soriano, S., Villa, P., Delagnes, A., Degano, I., Pollarolo, L., Lucejko, J. J., Henshilwood, C., and Wadley, L., 2015, The Still Bay and Howiesons Poort at Sibudu and Blombos: understanding Middle Stone Age technologies, *PLoS ONE*, **10**(7), e0131127.

Villa, P., Pollarolo, L., Degano, I., Birolo, L., Pasero, M., Biagioni, C., Douka, K., Vinciguerra, R., Lucejko, J. J., and Wadley, L., 2015, A milk and ochre paint mixture used 49,000 years ago at Sibudu, South Africa, *PLoS ONE*, **10**(6), e0131273.

Wadley, L., 2005, Putting ochre to the test: replication studies of adhesives that may have been used for hafting tools in the Middle Stone Age, *Journal of Human Evolution*, **49**(5), 587–601.

Wadley, L., 2007, Announcing a Still Bay industry at Sibudu Cave, South Africa, *Journal of Human Evolution*, **52**(6), 681–9.

Wadley, L., and Jacobs, Z., 2006, Sibudu Cave: background to the excavations, stratigraphy and dating, *Southern African Humanities*, **18**(1), 1–26.

Wadley, L., and Kempson, H., 2011, A review of rock studies for archaeologists, and an analysis of dolerite and hornfels from the Sibudu area, *KwaZulu-Natal, Southern African Humanities*, **23**, 87.

Wadley, L., and Lombard, M., 2007, Small things in perspective: the contribution of our blind tests to micro-residue studies on archaeological stone tools, *Journal of Archaeological Science*, **34**(6), 1001–10.

Wadley, L., Hodgskiss, T., and Grant, M., 2009, Implications for complex cognition from the hafting of tools with compound adhesives in the Middle Stone Age, South Africa, *Proceedings of the National Academy of Sciences*, **106**(24), 9590–4.

Wadley, L., Williamson, B., and Lombard, M., 2004, Ochre in hafting in Middle Stone Age Southern Africa: a practical role, *Antiquity*, **78**(301), 661–75.

Wadley, L., Trower, G., Backwell, L., and d'Errico, F., 2015, Traditional glue, adhesive and poison used for composite weapons by Ju/'hoan San in Nyae Nyae, Namibia: implications for the evolution of hunting equipment in prehistory, *PLoS ONE*, **10**(10), e0140269.

Wadley, L., Sievers, C., Bamford, M., Goldberg, P., Berna, F., and Miller, C., 2011, Middle Stone Age bedding construction and settlement patterns at Sibudu, South Africa, *Science*, **334**(60–1), 1388–91.

White, W. B., Vito, C., and Scheetz, B. E., 2009, The mineralogy and trace element chemistry of black manganese oxide deposits from caves, *Journal of Cave and Karst Studies*, **71**(2), 136–43.

Widjaja, E., and Sampanthar, J. T., 2007, The detection of laser-induced structural change of $MnO_2$ using *in situ* Raman spectroscopy combined with self-modeling curve resolution technique, *Analytica Chimica Acta*, **585**(2), 241–5.

Will, M., Bader, G. D., and Conard, N. J., 2014, Characterizing the Late Pleistocene MSA lithic technology of Sibudu, KwaZulu-Natal, South Africa, *PLoS ONE*, **9**(5), e98359.

Zupancich, A., Nunziante-Cesaro, S., Blasco, R., Rosell, J., Cristiani, E., Venditti, F., Lemorini, C., Barkai, R., and Gopher, A., 2016, Early evidence of stone tool use in bone working activities at Qesem Cave, *Israel, Scientific Reports*, **6**, 37686.

## SUPPORTING INFORMATION

Additional Supporting Information may be found online in the supporting information tab for this article.

Figure S1. Comparison between our residue mapping obtained by Raman micro-spectroscopy and SEM with that of microscopic observations by Lombard (2006).